*Journal of Physiology* (1995), **489.1**, *pp.*127–140


# Cellular mechanisms of 4-aminopyridine-induced synchronized after-discharges in the rat hippocampal slice

Roger D. Traub*†, Simon B. Colling‡ and John G. R. Jefferys‡

** IBM Research Division, T. J. Watson Research Center, Yorktown Heights, NY 10598, † Department of Neurology, Columbia University, New York, NY 10032, USA and ‡ Department of Physiology and Biophysics, St Mary's Hospital Medical School, Imperial College, London W2 1PG, UK*

1. We constructed a model of the *in vitro* rodent CA3 region with 128 pyramidal neurones and twenty-four inhibitory neurones. The model was used to analyse synchronized firing induced in the rat hippocampal slice by 4-aminopyridine (4-AP), a problem simultaneously studied in experiments in rat hippocampal slices. *N*-methyl-D-aspartate (NMDA) receptors were blocked.

2. Consistent with a known action of 4-AP, unitary EPSCs were assumed to be large and prolonged. With augmented EPSCs, spontaneous synchronized bursts occurred in the model if random ectopic axonal spikes were present. We observed probable antidromic spikes and miniature spikes experimentally.

3. Consistent with experiment, model synchronized bursts were preceded by a period of about 100 ms of increased unit activity and cell depolarization. In the model, this was caused in part by EPSPs consequent to ectopic axonal spikes.

4. After widespread firing had begun, full-blown synchrony in the model required orthodromic EPSPs. A single synchronized burst, once initiated, could proceed without further ectopic activity.

5. A depolarizing change in reversal potential for dendritic $GABA_A$ favoured the occurrence of synchronized after-discharges in the model. Consistent with this, bicuculline was found to *block* after-discharges in slices bathed in 4-AP (70 $\mu$M) during NMDA blockade.

6. These data indicate that, even with synaptic inhibition present, ectopic spikes can 'set the stage' for synchronized activity by depolarizing pyramidal cell dendrites, but that recurrent orthodromic EPSPs are required for expression of this synchrony. When synaptic inhibition is present, EPSCs may need to be larger than usual for synchrony to take place. Secondary bursts in 4-AP appear to be driven in part by a depolarizing $GABA_A$-mediated current.

A number of experimental manipulations, each altering synaptic and membrane properties in a distinctive manner, can induce epileptic after-discharges in hippocampal slices. While the biophysical mechanisms of the various manipulations are different, the neuronal population output is rather stereotyped: a series of synchronized population bursts, generally with the first burst longer than succeeding bursts. Why should this be? This question is important for the human epilepsies, where the underlying biophysical mechanisms are largely unknown, but whose principles might be revealed through study of features common to many diverse experimental epilepsies. In addition, the ready ability of groups of hippocampal neurones to produce population oscillations might be relevant to normal function.

To be specific, $GABA_A$ blockade, low extracellular concentrations of $Mg^{2+}$, and 4-aminopyridine (4-AP) at concentrations in the range of tens of micromolar, can all induce trains of synchronized bursts in rodent hippocampal slices (Miles, Wong & Traub, 1984; Ives & Jefferys, 1990; Avoli, Psarropoulou, Tancredi & Fueta, 1993; Traub, Jefferys & Whittington, 1994*b*). $GABA_A$ blockade cannot be the common mechanism, since evoked IPSCs are not completely blocked in low-$Mg^{2+}$ media (Whittington, Traub & Jefferys, 1995) and evoked IPSPs may even be increased in 4-AP (Buckle & Haas, 1982; Rutecki, Lebeda & Johnston, 1987). *N*-methyl-D-aspartate (NMDA) receptors are required for the later bursts in an after-discharge induced by $GABA_A$ blockade (Lee & Hablitz, 1990; Traub, Miles & Jefferys, 1993) – although not for the first burst –

and NMDA receptors are required for all synchronized activity in low-$Mg^{2+}$ media (Traub *et al.* 1994*b*). Yet NMDA receptors alone cannot be the common thread in the experimental epilepsies either, since prolonged synchronized bursts and after-discharges can be recorded in 4-AP during pharmacological NMDA blockade (Avoli *et al.* 1993); NMDA receptors are also not required for expression of after-discharges consequent to electrical stimulation (Stasheff, Anderson, Clark & Wilson, 1989). In this study we use experiments and computer simulations to explore how synchronized bursts and after-discharges might arise in 4-AP independent of NMDA receptors.

Relevant biophysical actions of 4-AP include the following. (1) Blockade of transient $K^+$ currents in postsynaptic soma–dendritic (SD) membrane, including the fast A current and the slower D current. Epileptogenic concentrations of 4-AP ($< 75\ \mu$M) probably do not block the A current (Storm, 1988). While such concentrations would be expected to block D current (Storm, 1988), our model neurones do not contain such a current. Hence, we did not simulate postsynaptic actions of the compound. (2) An increase in the excitability of axons (Kocsis, Ruiz & Waxman, 1983) and of presynaptic terminals (Buckle & Haas, 1982), probably also caused by $K^+$ current blockade, that would manifest itself as augmented release of neurotransmitter in response to presynaptic action potentials, and as spontaneous action potentials originating in terminals or in axons (Flores-Hernández, Galarraga, Pineda & Bargas, 1994). Secondary spill-over of GABA to extrasynaptic dendritic receptors could also cause the depolarizing bicuculline-sensitive potentials often observed in 4-AP (Perreault & Avoli, 1992). We did simulate these effects of 4-AP. We shall argue that augmented EPSCs, along with spontaneous axonal spikes, are sufficient to account for 4-AP-induced synchronized bursts during NMDA blockade. Depolarizing GABAergic currents in our model tend to convert single bursts into multiple bursts, and experimental data are consistent with this idea.

Some of the data in this paper were presented in preliminary form at the Brain Research Association meeting in Oxford, March 1995.

## METHODS

### Experimental methods

Adult male Sprague–Dawley rats from Harlan Olac (Bicester, UK), weighing 250–300 g, were stunned and then killed by cervical dislocation. Their brains were quickly removed, bisected along the mid-line and glued to the stage of a Vibroslice (Campden Instruments, Loughborough, UK). Sagittal hippocampal slices 500 $\mu$m thick were cut under cold ($< 8$ °C), freshly oxygenated artificial cerebrospinal fluid (ACSF) and transferred to an interface recording chamber maintained at 35 °C. The ACSF comprised (mM): 124 NaCl, 26 $NaHCO_3$, 5 KCl, 2 $CaCl_2$, 1·6 $MgCl_2$ and 10 glucose, equilibrated with a 95% $O_2$–5% $CO_2$ gas mixture, resulting in a pH of 7·4. Warm, wet gas mixture was directed over the surface of the slices.

Conventional microelectrode recording methods were used, from presumed pyramidal neurones in the CA3b/c region. Resting membrane potentials were −64·9 to −70·0 mV. Glass micropipettes for intracellular recording were filled with 2 M potassium acetate and had resistances of 60–100 MΩ. Extracellular recordings were taken using metal electrodes (stainless-steel wire; diameter, 125 $\mu$m). The recording system included an Axoclamp amplifier (Axon Instruments, Burlingame, CA, USA), Digitimer filters and a CED 1401–MSDOS computer system running SIGAVG and SPIKE2 (Cambridge Electronic Design Ltd, Cambridge, UK). Epileptic discharges were elicited by addition to the bath of 4-aminopyridine (4-AP, 70 $\mu$M). Drugs used to isolate components of the epileptic discharge were D-2-amino-5-phosphonopentanoic acid (AP5, 1–50 $\mu$M), 6-cyano-7-nitroquinoxaline-2,3-dione (CNQX, 20 $\mu$M), 6-nitro-7-sulphamoylbenzo(f)quinoxaline-2,3-dione (NBQX, 20 $\mu$M), 3-amino-2-(4-chlorophenyl)-2-hydroxypropylsulphonic acid (2OH-saclofen, 0·2 mM, Tocris, Bristol, UK), and bicuculline methiodide (1–30 $\mu$M).

### Simulation methods

**Approach to the network simulation.** The style of network simulation is similar to that used in previous studies of epileptogenesis in the CA3 region (e.g. Traub *et al.* 1993), with multiple pyramidal and inhibitory neurones interconnected by 'synapses' with 'receptors' intended to replicate AMPA (α-amino-3-hydroxy-5-methyl-4-isoxazole propionic acid), NMDA, $GABA_A$ and $GABA_B$ receptors. As before, neurones are represented as multicompartment objects, with several types of voltage- and $Ca^{2+}$-dependent membrane channels, and the goal remains the discovery of the simplest physiological principles that can account for available electrical records, and the posing of testable predictions. Nevertheless, the code has had to be entirely rewritten for the following reasons.

First, in 4-AP, there is evidence for the occurrence of antidromic action potentials, to replicate which the model pyramidal neurone must contain at least a section of axon. Dendritic IPSPs, especially if depolarizing, are also of likely relevance. Since synaptic contacts may, in principle, be patchy, a pyramidal model with branched dendrites could be useful (Gulyás, Miles, Hájos & Freund, 1993*a*; Buhl, Halasy & Somogyi, 1994). For these reasons, we employed a new branching dendritic CA3 pyramidal cell model (Traub, Jefferys, Miles, Whittington & Tóth, 1994*a*) with sixty-four soma–dendritic compartments, an initial segment (IS) and four unmyelinated axonal compartments.

Second, there is now evidence that CA3 pyramidal neurones can activate certain nearby inhibitory neurones recurrently via a single dendritic transmitter release site, with this remarkable synapse powerful enough that a single presynaptic action potential can often evoke a short-latency postsynaptic action potential (Miles, 1990; Gulyás, Miles, Sik, Tóth, Tamamaki & Freund, 1993*b*). In order to incorporate this finding, we have developed a branching dendritic model of an inhibitory interneurone and have found that spike-generating properties in the dendrites allow one EPSP, generated through a single synaptic site, to evoke an action potential (Traub & Miles, 1995). While this feature is not of clear significance for the 4-AP model, we have chosen to incorporate the more detailed interneurone

representation. In this way, the same network program can be used to simulate other types of population behaviour where spike-to-spike transduction may be important.

Third, in previous models, there were two types of inhibitory neurones: a type that produced '$GABA_A$' IPSPs at perisomatic locations and a type that produced '$GABA_B$' IPSPs in the apical dendrites. Since dendritic $GABA_A$-mediated inputs are of possible importance in 4-AP epileptogenesis (Perreault & Avoli, 1992) and since there is some anatomical information concerning synaptic contacts made by non-pyramidal neurones on pyramidal cell dendrites (Gulyás *et al.* 1993*a*; Buhl *et al.* 1994), we now include a separate type of inhibitory neurone, contacting sites in the apical dendrites. This latter neurone induces IPSCs whose time course is slower than for perisomatic IPSCs (Pearce, 1993; Miles, Tóth, Gulyás, Hajos & Freund, 1994), but whose time course is faster than for $GABA_B$ IPSCs. We also include inhibitory neurones that cause IPSCs on pyramidal neurone initial segments.

Fourth, the individual neurone models are now so complex that, for network simulations to be practical, a parallel computer is preferred. The code is therefore written for such a machine.

**General network structure.** There are 128 identical pyramidal neurones and twenty-four inhibitory neurones. The high interneurone : pyramidal neurone ratio is related to the small size of the network. There are five types of interneurones, all with identical intrinsic properties at this stage. Type 1 corresponds to chandelier cells whose contacts are restricted to the IS of pyramidal cells. Type 2 corresponds to basket cells with perisomatic synaptic contacts. Types 3 and 4 we call 'SR' cells, referring to sites of synaptic contact (stratum radiatum) rather than of presynaptic cell body, with type 3 contacting two particular compartments and type 4 contacting two other particular compartments. Type 5 cells cause $GABA_B$ IPSPs in apical dendrites. The sites at which synaptic contacts can be made on pyramidal neurones are shown in Fig. 1. There are four chandelier cells, eight basket cells, eight SR cells and four $GABA_B$ cells.

**Synaptic connectivity.** The synaptic connectivity is as follows. All connections are random. Each pyramidal cell and each interneurone receives synaptic input from thirty-two pyramidal cells. Each of these excitatory connections involves only a single compartment on the postsynaptic neurone, a feature supported by data for connections onto interneurones. The number of release sites for pyramidal-to-pyramidal connections is not yet established by anatomical techniques, but may be small (Traub & Miles, 1991). Excitatory contacts on interneurones are restricted to portions of the dendrites and do not occur on the soma. There are no interactions between interneurones in the present model, either via chemical synapses or via gap junctions.

Each pyramidal neurone receives synaptic input from two of the four chandelier cells, six of the eight basket cells (each contact onto four proximal basilar compartments, the soma and the apical shaft), two each from the two types of SR cells, and from all four $GABA_B$ cells.

**Model pyramidal neurones.** These are as described by Traub *et al.* (1994*a*), with a minor adjustment in the density of the after-hyperpolarization (AHP) conductance (multiplied by 0·75) and kinetics ($\alpha_q$, the forward rate function, multiplied by 2). This branching dendritic model includes six ionic conductances: $g_{Na}$, high-threshold non-inactivating $g_{Ca}$ and four $K^+$ conductances: the fast transient A conductance, delayed rectifier, the fast voltage- and $Ca^{2+}$-gated C conductance, and the slow $Ca^{2+}$-gated AHP conductance. The axon and IS contain $Na^+$ and delayed rectifier conductances only, and these conductances are of higher density than in the SD membrane. $Na^+$ channels in the SD membrane are concentrated at the soma and proximal dendrites, while $Ca^{2+}$ channels have highest density in mid-apical dendrites. The model pyramidal neurone was tested in several ways, including response to antidromic and orthodromic stimulation, response to steady currents injected into soma or apical dendrites, and by the interaction between dendritic bursts and dendritic IPSPs (Traub *et al.* 1994*a*).

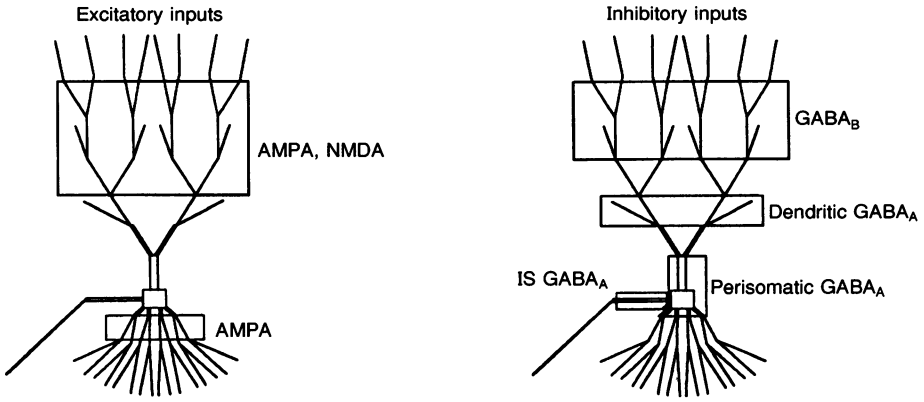


**Figure 1. Location of synaptic inputs on model pyramidal neurones**

Recurrent excitatory inputs activate AMPA receptors in the basilar and apical dendrites, and NMDA receptors in the apical dendrites. Recurrent IPSCs from 'chandelier cells' occur on the initial segment (IS; with time constant, 7 ms) and from 'basket cells' on the most proximal basilar dendrites, the soma and the apical shaft (also with time constant, 7 ms). IPSCs from dendritic $GABA_A$ neurones are in the middle apical dendrites (time constant, 50 ms). $GABA_B$ IPSCs are located more distally in the model.

**Model inhibitory neurones.** These are described more fully elsewhere (Traub & Miles, 1995). Each such cell has forty-six SD compartments, an IS and four axonal compartments. Conductances and kinetics are as for the pyramidal neurone but $g_{Ca}$ density is at most 1·0 mS cm$^{-2}$, so that firing behaviour is dominated by $g_{Na}$ and the delayed rectifier. $g_{Na}$ is 100 mS cm$^{-2}$ at the soma and can be 25 or 50 mS cm$^{-2}$ at selected locations in the dendrites. Passive parameters included the following: internal resistivity, $R_i = 200\ \Omega$ cm; membrane resisitivity, $R_m = 50\,000\ \Omega$ cm$^2$; membrane capacitance, $C_m = 0{\cdot}75\ \mu$F cm$^{-2}$; input resistance, $R_{input} = 98{\cdot}5$ MΩ; reversal potential for potassium conductance, $E_K = -25$ mV relative to resting potential. Depending on holding current, these model neurones may fire spontaneously, with little adaptation at high frequencies, but with some adaptation when near firing threshold. In the network, all $GABA_A$ interneurones are held with a −0·03 nA current that would lead (in the absence of synaptic inputs) to a steady firing rate of 10 Hz. $GABA_B$ cells are held with a −0·06 nA current, so that such cells do not fire when unstimulated.

**Synaptic interactions.** The essence of a network simulation, besides accurately modelling individual neurones, is to have a realistic representation of synaptic communication. In the present case, the representation must also involve as little message-passing as possible between the different computer processors on which the various neurones are being simulated. This is a non-trivial task, since the duration of synaptic actions is long (milliseconds to hundreds of milliseconds) compared with an integration time step (2·5 $\mu$s for pyramidal cells and 1·25 $\mu$s for interneurones). We have approached this problem as follows: a maximum amount of the computational work, associated with simulation of synaptic communication, is 'attached' to the presynaptic cell. In this way, messages can be passed between neurones relatively infrequently (we use a rate of 3·2 kHz). This approach is easiest to implement if all the synapses of a given type (say AMPA-mediated synapses at pyramidal-to-pyramidal connections) have the same 'weight' (amplitude scaling factor) and the same time course. Under such conditions, which we shall assume in the network model, axonal branching need not be simulated explicitly. Furthermore, the firing pattern of the most distal axonal compartment of each neurone can be used to determine the postsynaptic conductance, $g_{syn}$, which that presynaptic neurone generates in all of its connected postsynaptic neurones, thus fulfilling our technical requirement for concentrating the computational work on the presynaptic cell. After the $g_{syn}$ values are calculated, information about network connectivity allows the program to attach the correct synaptic conductances to appropriate compartments of the appropriate postsynaptic cells. Note that in this formalism, presynaptic terminals are not simulated as real entities, that is, there is no variable corresponding to the membrane voltage of the terminal, or the terminal $Ca^{2+}$ concentration. Rather, the terminal state is defined by the firing behaviour of the most distal axonal compartment.

The details of the formalism are as follows. Every 125 time steps (0·3125 ms), calculate $g_{syn}$ for all the neurones. (For pyramidal neurones, there are four types of $g_{syn}$ to calculate: the AMPA conductance produced on interneurones, the AMPA conductance produced on pyramidal neurones, and NMDA conductances produced respectively on interneurones and pyramidal neurones.) These $g_{syn}$ values are passed to postsynaptic neurones, and appropriate synaptic conductances are calculated for each compartment. Finally, saturation effects may be applied: that is, each compartment may be able to experience only a maximum conductance. The final compartmental synaptic conductance values can then be passed to the routines integrating the differential equations for each neurone. Within these routines, the voltage- and $Mg^{2+}$-dependent term for the NMDA conductance can also be calculated (as in Traub *et al.* 1994*b*). *NMDA conductances, however, were blocked in the present simulations*, except for calibrating runs: (1) to make sure the network model could replicate picrotoxin-induced after-discharges (Fig. 2; also see Traub *et al.* 1993); (2) to confirm that the network did not develop synchronous bursts when the AMPA conductance time course was in the control range, even with NMDA conductances present; and (3) to confirm that increasing AMPA conductances during the occurrence of ectopic spikes could lead to single synchronized bursts (rather than sustained after-discharges), even with NMDA conductances present, provided IPSCs were large enough.

For each type of neurone and synaptic action, $g_{syn}$ is defined by an equation of the following sort:

$$g_{syn} = \sum_{\tau} c \times Y(t - \tau)\, P(\tau),$$

where the sum is taken over all firing times, $\tau$, of the most distal axonal compartment of the presynaptic neurones, $c$ is a scaling constant, $Y$ is a function giving the time course of the unitary synaptic conductance, and $P$ is a function (dependent on the firing history of each presynaptic neurone) that scales the amount of transmitter released for each presynaptic spike. (Hence, $P$ can incorporate presynaptic facilitation and depression.) $t$ is the time in milliseconds and $\tau$ is, of course, also given in milliseconds.

It remains now only to define the various constants and functions. For scaling constants $c$, we used: 6 nS for AMPA onto a pyramidal cell apical compartment and 3 nS onto a basilar compartment; 8 nS for AMPA onto an interneurone dendrite; 6 nS for a $GABA_A$ synapse onto an initial segment; 20 nS, spread over six compartments in proportion to surface area, for a basket cell IPSC; either 10 or 20 nS for a dendritic $GABA_A$ IPSC, divided equally between two compartments; and 1 nS for a $GABA_B$ IPSC, spread over sixteen compartments in proportion to surface area. (Large synaptic conductances were used both to reflect the effect of 4-AP, as well as to correct for the unrealistically small number of inhibitory inputs per neurone; in addition, as seen below, there is presynaptic depression during high-frequency firing that diminishes synaptic efficacy.)

The unitary synaptic time courses are defined as follows. For an AMPA connection onto a pyramidal neurone, an $\alpha$ function is used: $Y(t) = te^{-t/\tau_{AMPA}}$, where $\tau_{AMPA}$ is 2 ms in control simulations, and is 3–5 ms in '4-AP' simulations. For an AMPA connection onto an interneurone, an $\alpha$ function is used with $\tau_{AMPA}$ of 1 ms. For $GABA_A$ connections on the IS or perisomatic regions, $Y(t) = e^{-t/7}$. For dendritic $GABA_A$, $Y(t) = e^{-t/50}$ (Pearce, 1993; Traub *et al.* 1994*a*). For $GABA_B$ connections, we used the time course specified by Otis, de Koninck & Mody (1993) (see also Traub *et al.* 1994*a*).

The weighting functions $P$ take on the value 1·0 at the start of each simulation. For a pyramidal cell 'terminal' (onto either another pyramidal cell or an interneurone) transient facilitation up to a value of 2 occurs, then depression (down to $P = 0{\cdot}2$). If the previous axonal spike occurred less than 4 ms in the past, $P = 0$ (to simulate terminal refractoriness, although the exact value of

this parameter is not known). Otherwise, terminals facilitate or depress if interspike intervals are < 10 ms, and they recover when intervals are >25 ms. Inhibitory terminals do not facilitate, but exhibit depression only (to $P = 0{\cdot}2$) when firing occurs at 100 Hz or faster, with recovery when the axon is quiet for 200 ms. Note that terminal behaviour is influenced not only by somatic spikes propagating forward, but also by random ectopic spikes originating in the axon (see below).

Saturating conductances for each postsynaptic compartment are as follows: 5 nS for AMPA on pyramidal basilar and interneuronal dendrites; 15 nS for AMPA on pyramidal apical dendrites; and 0·15 nS for $GABA_B$ on pyramidal apical dendrites. $GABA_A$ conductances do not saturate in this model.

Reversal potentials for synaptic conductances are (relative to resting potential): +60 mV for EPSPs; and −15 mV for $GABA_B$ and $GABA_A$ IPSPs on the IS and perisomatic regions. Dendritic $GABA_A$ reversal potential was −15 mV unless specified otherwise.

**Ectopic axonal action potentials.** These were generated in the model by a random Poisson process applied independently to each pyramidal cell axon, with mean interval '$T_{ectopic}$' from 10 ms to 1 s. The stimulus used was a 0·2 nA, 0·3125 ms current pulse applied to the most distal axonal compartment. This was easily sufficient to evoke an action potential. The ectopic spike might or might not invade the soma, depending on IS and perisomatic membrane conductances (see Results). One reason for using ectopic spikes as a source of synaptic potentials (rather than 'spontaneous' transmitter release) is that, in 4-AP, synaptic potentials are largely blocked by tetrodotoxin (Perreault & Avoli, 1991).

**The parallel simulation algorithm.** Simulations were run on an IBM 9076 SP1 parallel computer. This machine consists of a collection of 'nodes' (each comparable to a high-performance workstation) that are interconnected by a high-speed switch. The switch permits all-to-all communication between the nodes, but because of overhead associated with its use, one tries not to have node-to-node communication too often. The program ran on either eight or sixteen nodes. In the eight-node version, sixteen pyramidal neurones and three interneurones were first assigned to each node. The cells were initialized exactly as in single neurone simulations. Each node then constructed an identical wiring diagram of the network (which cell is connected to which other cells at which postsynaptic compartments). Various parameters were set, such as holding currents, ectopic spike frequency, $\tau_{AMPA}$ and dendritic $GABA_A$ reversal potential. The simulation proper then cycled through the following steps. (1) Given the values of $g_{syn}$ for all 'presynaptic terminals' (more precisely, the most distal axonal compartment), calculate postsynaptic conductances for all the neurones on each node. This uses the wiring diagram, an identical copy of which resides on each node. (2) Generate random current pulses in the distal axons. (3) Using the synaptic conductances and current inputs, along with the present membrane state variables, integrate the differential equations for the neurones for 125 time steps (0·3125 ms). (4) Calculate new values of $g_{syn}$, as described above. (5) Each node broadcasts the $g_{syn}$ values for its neurones to all of the other nodes. (6) Repeat.

**Test of the model: $GABA_A$ blockade.** When $GABA_A$ conductances were set to zero, and NMDA conductances were large enough, the network model would generate a synchronized after-discharge (Fig. 2), resembling experimental recordings and the results of an earlier network model (Traub *et al.* 1993). In the present case, however, the after-discharges tended to persist indefinitely, unless NMDA conductances were very precisely tuned. This observation raises the possibility of NMDA desensitization during $GABA_A$ blockade, as has been suggested for low-$Mg^{2+}$ after-discharges (Traub *et al.* 1994*b*); other factors (such as voltage- or $Ca^{2+}$-dependent inactivation of dendritic $g_{Ca}$) could also be important in terminating the after-discharge, however.

**Preliminary simulations.** Preliminary simulations of 4-AP-induced bursts with a large network model have been performed. The large network contains 1024 pyramidal neurones and 256 interneurones (32 axo-axonic, 64 basket cells, 32 cells eliciting $GABA_A$ IPSPs on pyramidal cell dendrites and 128 cells eliciting

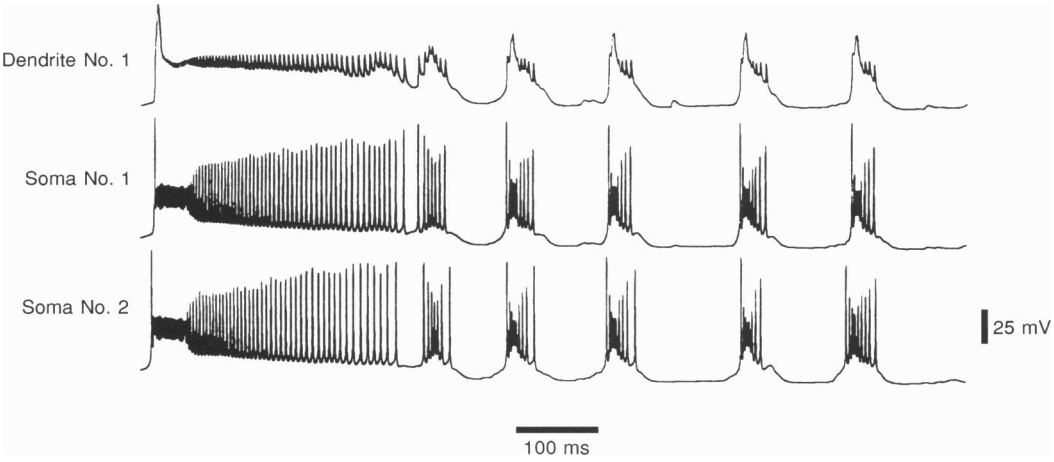


**Figure 2. Simulation of picrotoxin effects: a test of the model**

The network model produces synchronized after-discharges when NMDA receptors are active and $GABA_A$ receptors (on initial segment, perisomatic region and apical dendrites) are blocked. This behaviour is consistent with experiment and with a previous model (Miles *et al.* 1984; Traub *et al.* 1993). Saturating NMDA conductance is 25 nS per compartment, 500 nS total. Dendritic potential from a site in apical dendrites centred 240 $\mu$m from soma of a pyramidal neurone.

$GABA_B$ IPSPs). The qualitative behaviour of the large network is similar to the behaviour of the smaller network described here.

**Computing requirements.** Simulation programmes were written in FORTRAN, augmented by parallel instructions (e.g. mp_concat for broadcasting data) by R.D.T. and run on an IBM 9076 SP1 parallel computer. A simulation of 1000 ms of 'neuronal time', running on sixteen nodes, used about 2–2·5 h of computer time. For questions on programming details, the reader should send electronic mail to R.D.T. at TRAUB@YKTVMV.BITNET or traub@watson.ibm.com.

## RESULTS

### Simulation of synchronized burst induced by 4-AP with NMDA blockade

When $\tau_{AMPA}$ was 2 ms, synchronized bursts did not occur in the model, even with $T_{ectopic}$ as short as 10 ms (not shown). When $T_{ectopic}$ was 80 ms, the threshold $\tau_{AMPA}$ for synchronization to develop was between 2·7 and 2·8 ms. Figure 3 illustrates a simulated synchronized burst when $\tau_{AMPA}$ is 3·0 ms. For two pyramidal neurones, we plot the potential at three different sites, thereby allowing discrimination between ectopic axonal spikes and orthodromic spikes. In this figure, ectopic axonal spikes may produce: (a) minimal voltage deflections at the soma (when the latter is hyperpolarized); (b) partial spikes or 'd-spikes' ('d' in the figure); or (c) an antidromic spike ('a') with a prominent inflexion on its rising phase. An orthrodromic spike ('o') also occurred, preceded by an EPSP. The population burst has, as expected, a depolarizing envelope at the soma. The two cells illustrated also exhibit IPSPs just before the burst, as can happen experimentally (Rutecki *et al.* 1987). It is not immediately apparent from this illustration how or why synchrony develops when it does; we shall return to this question below.

### Ectopic axonal spikes

Characteristics of presumed ectopic axonal spikes in CA3 pyramidal neurones have been described by Stasheff, Hines & Wilson (1993*a*) and Stasheff, Mott & Wilson (1993*b*). Figure 4 shows details of some of the pyramidal cell action potentials from the simulation of Fig. 3. In Fig. 4*A–D*, a 'spontaneous' axonal spike occurs first. As the axonal spike

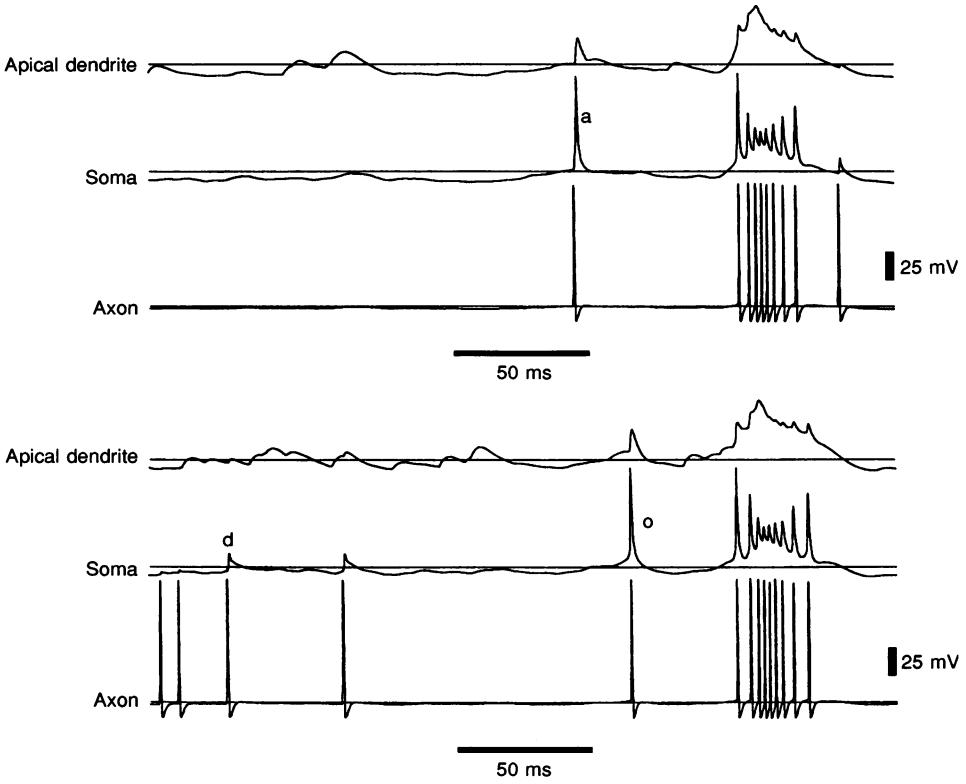


**Figure 3. '4-AP–AP5' simulation: membrane events in pyramidal neurones before synchronized burst**

For each of 2 pyramidal cells, we plot the potential at an apical dendritic site (240 $\mu$m from the soma), at the soma, and at the most distal axonal compartment. EPSPs are most prominent in the dendrite. Spontaneous ectopic axonal spikes may fail to invade the soma fully, causing miniature axon potentials (partial spikes or d-spikes, 'd'), or invade to produce an antidromic spike ('a') that rises abruptly and has an inflected rising phase (see also Fig. 4). Orthodromic spikes ('o') also occur just before the synchronized burst, arising from a membrane depolarization (note the dendritic EPSP). $\tau_{AMPA} = 3$ ms; $T_{ectopic} = 80$ ms; dendritic $GABA_A$ scaling parameter, 20 nS.

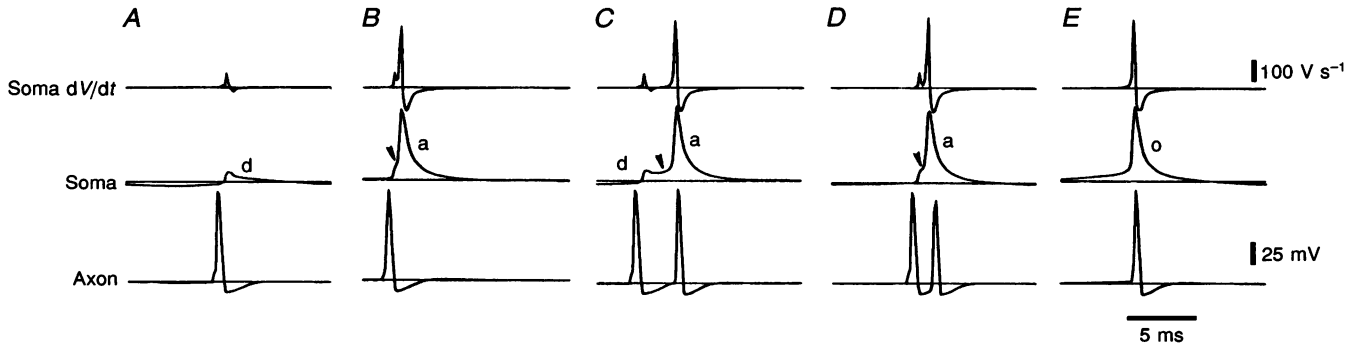


**Figure 4. Detailed morphology of simulated action potentials**

Same simulation as Fig. 3 ('4-AP–AP5'). Events were chosen from different pyramidal cells. Events *A–D* are of ectopic origin, while event *E* is orthodromic. The antidromic spike may fail and cause a somatic partial spike ('d') or fast prepotential (*A*), or cause a somatic spike ('a'), starting to rise abruptly but with an inflected rising phase (arrowheads), corresponding to a dip in the d*V*/d*t* signal (*B–D*). A reflected spike can occur, whose latency depends on the timing of somatic invasion by the antidromic spike (*C–D*). Orthodromic spikes ('o') arise from a gradual somatic depolarization and are not inflected (*E*). Compare Fig. 5, and Stasheff & Wilson (1990, their Fig. 1), as well as Stasheff *et al.* (1993*a*).

invades the soma, a potential of 15–20 mV occurs, with d*V*/d*t* about 50 V $s^{-1}$. This somatic potential may occur in isolation (Fig. 4*A*); it may blend into a full somatic spike, appearing as an inflexion (Fig. 4*B* and *D*); or it may cause a somatic spike after a delay of a few milliseconds (Fig. 4*C*). The full somatic spike is associated in the model with a d*V*/d*t* of about 200 V $s^{-1}$. In some cases, a second 'reflected' axonal spike is generated (Fig. 4*C* and *D*). There is experimental evidence for such reflected spikes after evoked antidromic action potentials (Traub *et al.* 1994*a*), but data are lacking on this point in 4-AP. Note that the orthodromic spike (Fig. 4*E*) rises from a somatic depolarization and is not preceded by a prepotential or a notch in the d*V*/d*t* trace.

Action potentials and prepotentials similar to those of Fig. 4*A*, *B* and *E* have been reported by Stasheff & Wilson (1990) in hippocampal slices developing epileptiform activity after repetitive electrical stimulation. Figure 5 documents that similar events occur in 4-AP (70 μM), AP5 (20 μM), saclofen (200 μM) and NBQX (20 μM), typically occurring at intervals of about 20 s. AMPA receptor antagonists blocked orthodromic spikes. These data suggest that ectopic axonal spikes do, indeed, occur in 4-AP.

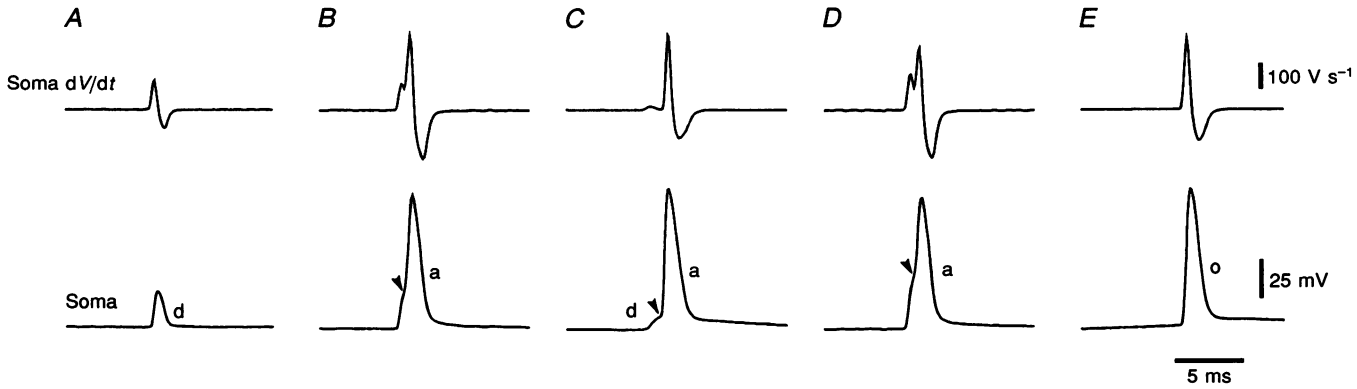


**Figure 5. Experimental spontaneous action potentials recorded from the soma, along with the corresponding d*V*/d*t* signal**

Events *A–D* are presumed to be of ectopic antidromic origin and were recorded from the soma in the presence of 70 μM 4-AP, 20 μM AP5, 200 μM 2OH-saclofen and 20 μM NBQX. They show partial ('d') spikes (*A* and *C*), full somatic spikes ('a' in *B–D*), and a delayed action potential (*C*). Note that experimental recordings were not taken from the axon. A presumed orthodromic action potential is shown in *E*, obtained in the absence of NBQX. Spikes with an inflected rising phase (arrowheads, *B–D*), characteristic of ectopic action potentials, were abolished by 30 μM bicuculline methiodide (data not shown).

Bicuculline methiodide (30 $\mu$M) suppressed the ectopic spikes in 4-AP (data not shown), as occurs also after electrical stimulation (Stasheff *et al.* 1993*b*).

**Build-up of activity before synchronized burst**

Figure 6 indicates that the network model exhibits a build-up of activity in the 100 ms before a synchronized burst, despite the constant mean frequency of ectopic axonal spikes. This build-up can be seen in: (a) a progressive membrane depolarization, apparent in the average potentials at dendritic or somatic sites, although not always in individual cells (Fig. 3); or (b) an increase in pyramidal cell 'unit activity'. Experimentally, both somatic depolarization and increased unit activity have been recorded in the 100 ms before a synchronized burst in 4-AP (Ives & Jefferys, 1990). In the network model, this behaviour occurs because, as the burst AHPs fade, sufficiently large ectopic EPSPs (EPSPs caused by 'forward' propagation of ectopic spikes) can depolarize pyramidal cell membranes above resting potential. Such depolarization has several effects: first, it allows ectopic spikes to invade the soma and increases the probability of reflected spikes, thereby providing amplification; and, second, sufficient membrane depolarization leads to orthodromic spikes. Eventually, this regenerative activity leads to bursting in all the neurones.

A formally similar model has been suggested for the regenerative build-up to synchrony in high-[$K^+$]-induced bursts (Traub & Dingledine, 1990), although it was increased EPSP frequency that was monitored rather than unit activity (Chamberlin, Traub & Dingledine, 1990). In addition, ectopic spikes were not simulated but rather random EPSPs. The similarity lies in the progressive cell depolarization by 'background' EPSPs causing cell firing, further EPSPs etc. leading to a population burst. The regenerative nature of this process was illustrated by synaptically disconnecting the cells (Fig. 5 in Traub & Dingledine, 1990). A similar simulation (Fig. 7) helps to elucidate the relative roles of ectopic and orthodromic spikes in the 4-AP model. The 'control' potential is the soma of a pyramidal neurone from the same simulation as Figs 3 and 4. The simulation was repeated with sudden perturbations at the time of acceleration of the synchronization process (large arrowheads). When ectopic

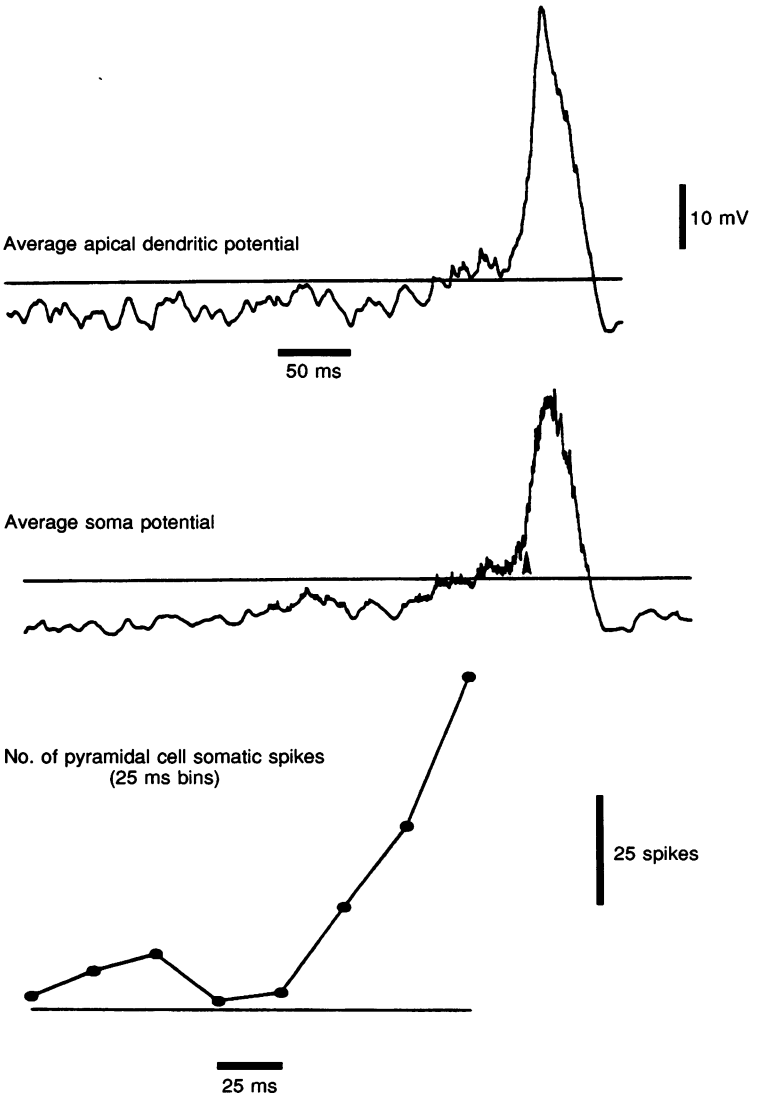


**Figure 6. Build-up of population activity before simulated synchronized burst**

Same simulation as Fig. 3 ('4-AP–AP5'). Beginning about 100 ms before the synchronized event (large waves), the build-up can be seen as a gradual dendritic depolarization (average of 16 pyramidal neurones at a site 240 $\mu$m from the soma), as a gradual somatic depolarization (average of all 128 pyramidal neurones), or as an increase in 'unit activity' (cf. Ives & Jefferys, 1990). 'Unit activity' was computed by counting all somatic spikes, in all 128 pyramidal neurones, in 25 ms bins going backwards from the inflexion on the mean somatic potential (arrowhead in middle trace). As the rate of ectopic spikes is constant on average, the build-up in 'unit activity' must reflect either increasing numbers of orthodromic spikes, or increased probability that ectopic spikes successfully invade the soma, or both.

spikes are stopped abruptly (after the build-up has begun), the synchronized burst continues virtually unchanged (Fig. 7, middle trace). (Without ectopic spikes at all, the synchronized burst does not occur; not shown.) Population behaviour is quite different when the cells are disconnected, by setting the soma–IS conductance to zero in all pyramidal cells abruptly (Fig. 7, bottom trace). Such a manipulation allows the cells to fire, but orthodromic communication becomes impossible; on the other hand, ectopic spikes can still produce EPSPs. In this case, full bursts do not occur.

We interpret Fig. 7 as follows. In our model, ectopic spikes produce EPSPs that begin to cause orthodromic firing and the beginning of population synchrony. After that point, orthodromic communication between neurones is essential for full synchrony to develop, whereas ectopic spikes are no longer required.

### After-discharges in 4-AP with NMDA blockade

In hippocampal slices from immature animals (Avoli *et al.* 1993), or in mature slices in 5·0 mM $K^+$ (Fig. 8), 4-AP can induce synchronized after-discharges. Strikingly, such after-discharges occur in 4-AP during NMDA blockade, either with 20 $\mu$M AP5 (Fig. 8*B*), or with 50 $\mu$M AP5 (not shown). Spontaneous events during NMDA blockade take place at about 1 $min^{-1}$; the frequency of secondary bursts in Fig. 8*B* is about 6 Hz (average, 6·5 ± 1·0 Hz *vs.* 5·6 ± 0·3 Hz in 4-AP alone; means ± S.E.M.; see Fig. 9). This is in contrast to the situation during $GABA_A$ blockade (Lee & Hablitz, 1990; Traub *et al.* 1993) or in low $Mg^{2+}$ (Traub *et al.* 1994*b*), in both of which cases NMDA receptors are required for bursts following the initial burst (and for the initial burst as well in low $Mg^{2+}$).

What might sustain the after-discharges in 4-AP? Several factors could contribute, including elevated extracellular $[K^+]$, prolonged AMPA-mediated EPSCs, depolarizing $GABA_A$ currents (as suggested by Perreault & Avoli, 1992), and ectopic axonal bursts of action potentials or high-frequency ectopic spikes. The data in Fig. 8*C* show that the secondary bursts in 4-AP are significantly reduced in number by bicuculline (30 $\mu$M) under conditions of simultaneous NMDA receptor blockade. This suggests that a depolarizing $GABA_A$-induced current may 'drive' the secondary bursts. In addition, the occurrence of spontaneous synchronized bursts in bicuculline (at about one every 5 s) indicates that some source of spontaneous excitation (other

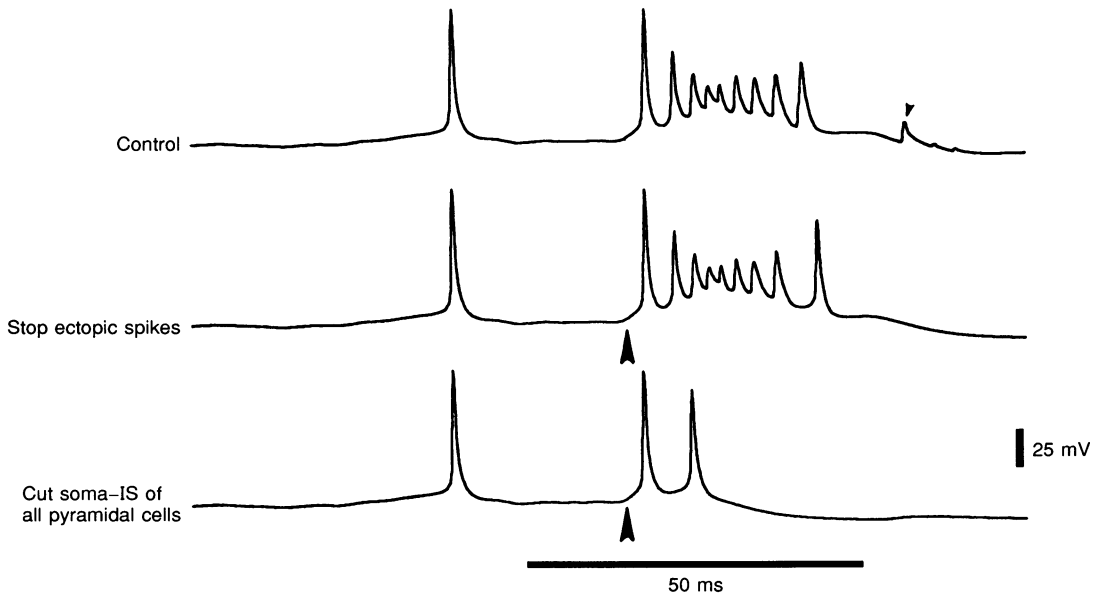


**Figure 7. Synchrony requires orthodromic EPSPs**

Once the simulated synchronized burst is underway, it continues without ectopic axonal spikes, but quickly attenuates if orthodromic activity is blocked. Control (top) is somatic potential of pyramidal neurone from the simulation of Fig. 3 ('4-AP–AP5'; $\tau_{AMPA} = 3$ ms, $T_{ectopic} = 80$ ms). The burst is part of a population burst since it appears almost simultaneously in all pyramidal cells (not shown). Middle trace: the simulation was repeated, but at the time marked by the large arrowhead, the probability of ectopic spikes was set to zero (note the absent partial spike that is present in the control run; small arrowhead). In this case, the synchronized burst still occurs. Bottom trace: the simulation was again repeated, but at the time marked by the large arrowhead, the coupling conductance between initial segment and soma, for all pyramidal neurones, was set to zero. Neurones can still fire (albeit with somewhat elevated threshold), but somatic spikes are unable to influence other neurones. In contrast, ectopic spikes can still produce EPSPs by forward propagation (although they cannot produce antidromic spikes or partial spikes). Thus, with the present synaptic and axonal parameters, ectopic spikes cannot by themselves *support* the population burst, even though they help to initiate it.

than ectopic spikes, which are blocked by bicuculline) must exist in 4-AP; perhaps some degree of spontaneous transmitter release is favoured by the 5 mM $[K^+]$.

The observations shown in Fig. 8 are quantificated in Fig. 9, using data collected from nine slices. In 4-AP alone, there were 12·6 ± 2·2 after-discharges, not significantly different from the 15·0 ± 3·4 after-discharges in 4-AP + AP5 (20 μM). In 4-AP + AP5 + bicuculline (30 μM), there were 5·4 ± 0·7 after-discharges, significantly fewer than in 4-AP alone or in 4-AP + AP5 ($p < 0·003$).

The action of $GABA_A$ receptors in generating after-discharges in 4-AP is not an *exclusive* one. Thus, secondary bursts can occur in 70 μM 4-AP in the presence of 30 μM bicuculline, provided NMDA receptors are not blocked (data not shown). Apparently, then, NMDA receptors alone *or* $GABA_A$ receptors alone can 'drive' the after-discharge in 4-AP, and the different receptors probably act synergistically.

We explored with the network model a possible role of depolarizing $GABA_A$-induced currents. In Fig. 10, the traces were from simulations with identical parameters

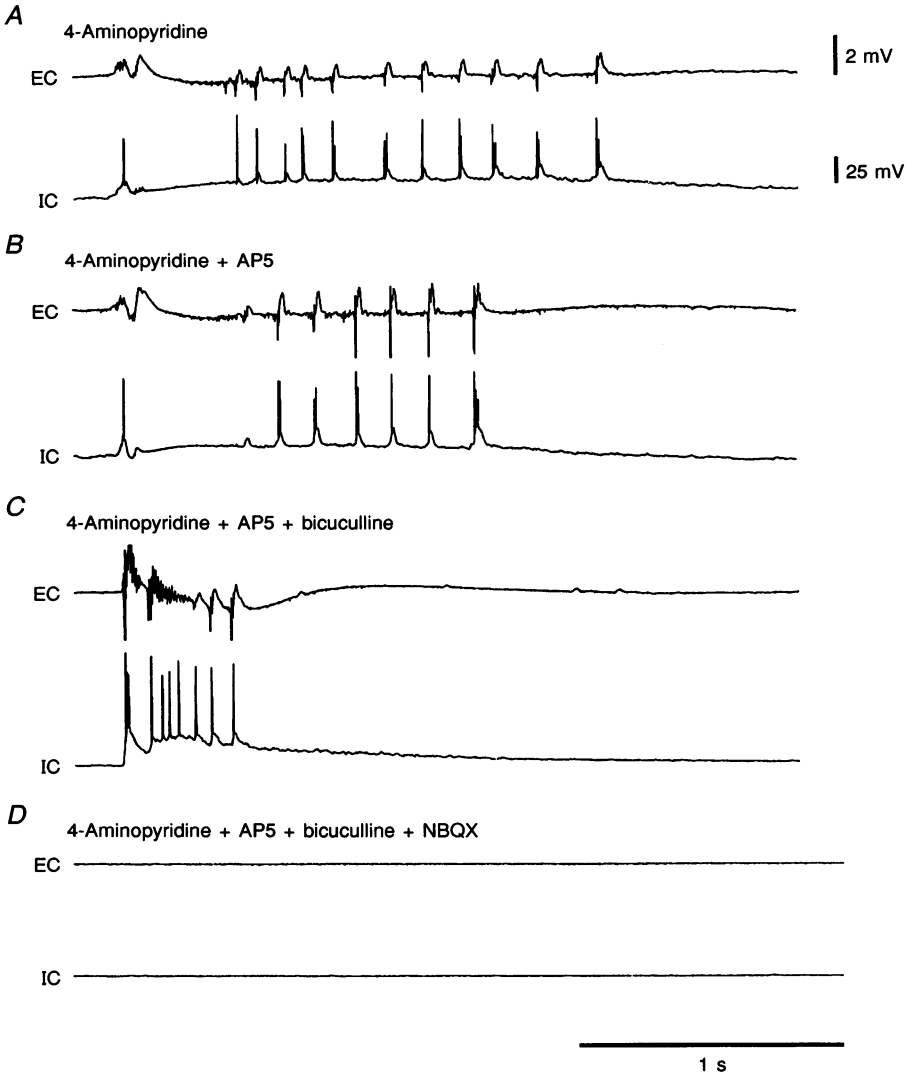


**Figure 8. Experimental spontaneous after-discharges in 4-AP occur during NMDA blockade, but are attenuated by $GABA_A$ blockade**

Simultaneous intracellular (IC) and extracellular (EC) recordings show both primary bursts and after-discharges in the presence of 70 μM 4-AP (*A*). The after-discharges remained following NMDA receptor blockade by 20 μM AP5 (*B*), showing that NMDA receptors are not required for these later events in the 4-AP experimental model. (The after-discharges also remained following 50 μM AP5; not shown.) $GABA_A$ receptor blockade by 30 μM bicuculline methiodide resulted in attenuation of the after-discharges (*C*), leaving a primary burst sometimes followed by more compact secondary events. Spontaneous synchronous activity was abolished by the further addition of 20 μM NBQX (*D*), although single action potentials were occasionally recorded. See Fig. 9 for quantification of these results.

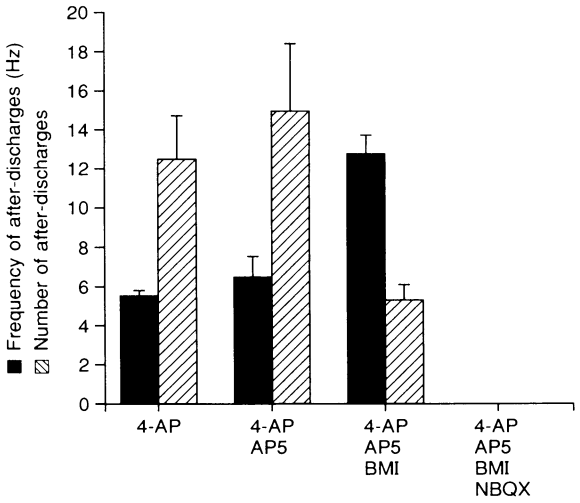


**Figure 9. Frequency and number of after-discharges under the various experimental conditions**

4-AP (70 $\mu$M) resulted in after-discharges, the number and frequency of which were not dependent on NMDA receptors, shown by the addition of 20 $\mu$M AP5. Bicuculline methiodide (BMI; 30 $\mu$M) attenuated the after-discharges, leaving secondary events significantly lower in number ($p < 0{\cdot}003$ compared with 4-AP + AP5) and higher in frequency ($p < 0{\cdot}0001$). These secondary events were abolished by NBQX (20 $\mu$M). Values are means ± S.E.M.

except for the reversal potential for dendritic $GABA_A$ conductances ($E_{GABA_A}$). This figure indicates that, provided ectopic spikes occur frequently enough ($T_{ectopic} = 30$ ms), a depolarizing $GABA_A$ conductance can elicit repeating dendritic bursts. The dendritic $GABA_A$ conductance is sustained not only by the postulated 50 ms time constant for dendritic IPSC decay (Pearce, 1993), but also because inhibitory neurones fire at high frequency during the after-discharge (not shown). We did not observe after-discharges in the network model, using the parameters of Fig. 10 with less frequent ectopic spikes (e.g. $T_{ectopic} = 80$ ms, not shown).

## DISCUSSION

### Initiation of the synchronized burst in 4-AP; analogy with high-[$K^+$] epileptogenesis

The initiation of a synchronized burst requires that firing spread from neurone to neurone. The fact that synaptic inhibition appears to be increased in 4-AP (Rutecki *et al.* 1987) makes such spread problematical. While synaptic excitation is also increased in 4-AP (Rutecki *et al.* 1987), it is not clear that excitation is strong enough to permit synchronization, particularly of spontaneous population bursts, without other factors. We propose a mechanism analogous to an earlier model of high-[$K^+$] epileptogenesis (Traub & Dingledine, 1990): with a constant background of excitatory synaptic 'noise', there is a build-up of cellular depolarization that accelerates and becomes regenerative in the 100 ms or so before full synchronization. The build-up is experimentally apparent as an increase in unit activity (Ives & Jefferys, 1990) or EPSP frequency (Chamberlin *et al.* 1990). In effect, the cells become depolarized enough so that, with increased excitatory synaptic conductance (or reduced inhibitory efficacy in the case of high [$K^+$]), firing can spread from cell to cell.

### Ectopic spikes

In the present model, ectopic spikes provide the random excitatory noise. Ectopic spikes occur in 4-AP (Fig. 5) and

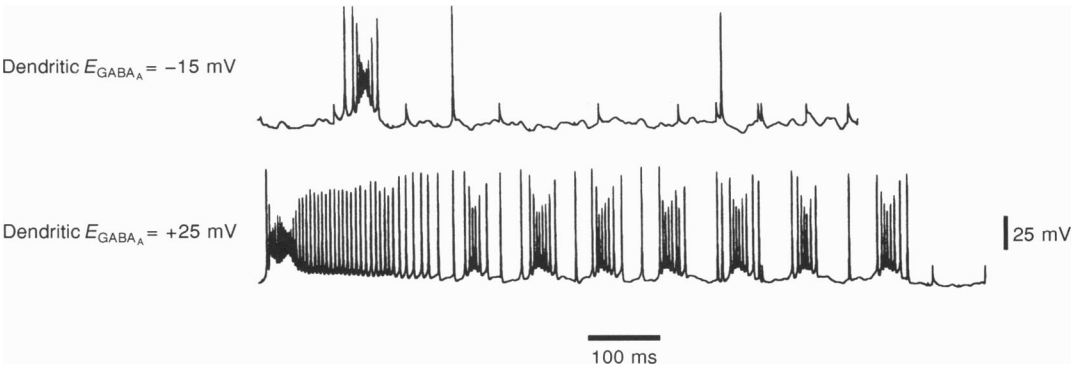


**Figure 10. After-discharges could result from depolarizing dendritic GABA conductance**

In the model, if the reversal potential of dendritic $GABA_A$ IPSPs is depolarizing, the net effect is excitatory, so that single synchronized bursts are converted into sustained after-discharges, without NMDA receptors. '4-AP–AP5' model with $\tau_{AMPA} = 3$ ms; $T_{ectopic} = 30$ ms; dendritic $GABA_A$ scaling parameter, 20 nS. Reversal potentials are given relative to the membrane resting potential.

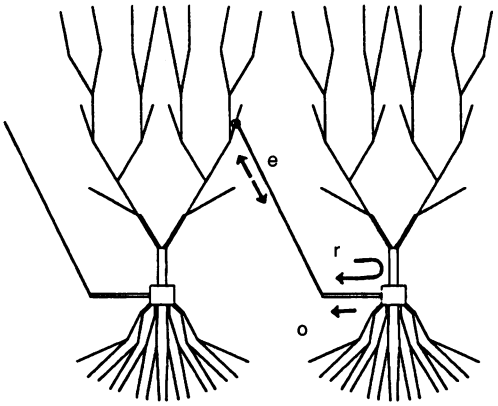


**Figure 11. Possible modes of pyramidal cell intercommunication in the present model**

Axonal branching not shown. Orthodromic spikes ('o') propagate forward to postsynaptic neurones. Ectopic spikes ('e') from axons or presynaptic terminals propagate *forward* to synaptic terminals or *retrograde* to cell body, where partial spikes or antidromic spikes can be observed. Sometimes, antidromic firing results in reflected spikes ('r'), or even bursts, that might propagate forward to re-activate synaptic terminals. The present model does not exhibit spontaneous bursts of action potentials generated entirely in axons, and axonal branching is not simulated explicitly (although the distal axon of any one model pyramidal neurone synaptically influences many other pyramidal neurones and inhibitory cells).

would be TTX sensitive, as is most of the synaptic noise in 4-AP (Perreault & Avoli, 1992). Interestingly, ectopic spikes in 4-AP are bicuculline sensitive, as is true also of ectopic spikes after electrical stimulation (Stasheff *et al.* 1993*b*). Ectopic spikes provide a 'drive' to the neuronal network in several ways (Fig. 11). First, by directly invading presynaptic terminals, they release glutamate onto one or more postsynaptic neurones. Second, they can generate antidromic spikes (Gutnick & Prince, 1972) that may even propagate into dendrites (Traub *et al.* 1994*a*). Finally, they might produce reflected spikes that would re-invade presynaptic terminals; such a phenomenon has been demonstrated in 'normal' media (Traub *et al.* 1994*a*), but we do not know if it occurs in 4-AP.

The mean frequency of ectopic spikes in our model ($T_{ectopic}$ of 80 ms corresponding to 12·5 Hz) may be unrealistically high, but the true frequency of ectopic spikes is difficult to determine experimentally with somatic recordings: ectopic spikes may fail to invade the soma (Fig. 3). In preliminary simulations of a large network (1024 pyramidal neurones and 256 interneurones), we found that synchronized bursts could occur with $T_{ectopic}$ as long as 5 s, provided $\tau_{AMPA}$ was 4 ms and unitary IPSCs were not too large (e.g. 3 nS for basket cell IPSCs) (R. D. Traub, S. B. Colling & J. G. R. Jefferys, unpublished observations). The interdependence of network size, ectopic spike frequency and synaptic inhibition is clearly important to analyse, but the long duration of the calculations makes a systematic exploration of the parameter space difficult (about 12 h of central processing unit (CPU) time on sixteen nodes for the above large network).

Spontaneous synchronized bursts occur in 4-AP with bicuculline and AP5, as of course they do in bicuculline alone. Since bicuculline appears to suppress ectopic spikes, there must be alternative sources of background 'drive'. Such sources could include TTX-sensitive transmitter release or intrinsic membrane events.

### Mechanism of secondary bursts

Unlike the situation during $GABA_A$ blockade or in low $Mg^{2+}$, secondary bursts in 4-AP do not require NMDA receptors (Fig. 8). Interestingly, this is also the case with after-discharges induced by electrical stimulation, in which ectopic spikes occur likewise (Stasheff *et al.* 1989, 1993*a*). Avoli and colleagues have described a long-lasting depolarizing $GABA_A$-mediated potential on the trailing end of 4-AP-induced synchronized bursts (e.g. Perreault & Avoli, 1992), and our data suggest that such a potential can drive secondary bursts in the CA3 region. In our network model, a reversal potential for dendritic $GABA_A$ only 25 mV positive to resting potential would suffice, provided ectopic spikes occur often enough. Indeed, we found that with a $T_{ectopic}$ of 30 ms, and $\tau_{AMPA}$ of 5 ms, secondary bursts could occur even without depolarizing $GABA_A$ actions and with NMDA blockade (data not shown). On the other hand, preliminary simulations in the larger network (1024 pyramidal cells and 256 inhibitory cells) show that secondary bursts driven by depolarizing $GABA_A$ actions do not require a high frequency of ectopic spikes, providing dendritic $GABA_A$ IPSCs decay slowly enough (e.g. with time constant 100 ms rather than 50 ms; data not shown). Since depolarizing $GABA_A$ receptors and ectopic spikes are both blocked by bicuculline, experimental dissection of the two mechanisms may be difficult. Electrically induced ictal events are also suppressed by bicuculline (Stasheff *et al.* 1993*b*), but the same ambiguity obtains: is the suppression due to loss of ectopic spikes, to blockade of a depolarizing $GABA_A$ action, or both?

### Unifying principles in experimental after-discharges

Based on experimental/modelling studies of three types of after-discharges ($GABA_A$ blockade: Traub *et al.* 1993; low $Mg^{2+}$: Traub *et al.* 1994*b*; and 4-AP: present data), we propose the following unifying principles that these after-discharges have in common: (1) intrinsic properties of pyramidal cells, most importantly the ability of dendrites

to generate repeating bursts in response to a tonic inward current; (2) recurrent excitatory collaterals (Miles & Wong, 1987) that allow spread of firing to occur and that can maintain synchrony of the secondary bursts; and (3) a source of tonic dendritic input that engages principle (1) above. During $GABA_A$ blockade and in low $Mg^{2+}$, such dendritic input involves massive glutamate release and opening of NMDA receptor–channels. In 4-AP, the drive apparently involves, at least in part, a postsynaptic depolarizing $GABA_A$ action, although high-frequency ectopic spikes could conceivably also contribute.

It will be interesting to see if the principles apply to electrically induced as well as other types of after-discharge. The principles do not apply, however, to all types of experimental epileptogenesis, since field-bursts do not depend on chemical synapses (Haas & Jefferys, 1984).


Avoli, M., Psarropoulou, C., Tancredi, V. & Fueta, Y. (1993). On the synchronous activity induced by 4-aminopyridine in the CA3 subfield of juvenile rat hippocampus. *Journal of Neurophysiology* **70**, 1018–1029.

Buckle, P. J. & Haas, H. L. (1982). Enhancement of synaptic transmission by 4-aminopyridine in hippocampal slices of the rat. *Journal of Physiology* **326**, 109–122.

Buhl, E. H., Halasy, K. & Somogyi, P. (1994). Diverse sources of hippocampal unitary inhibitory postsynaptic potentials and the number of synaptic release sites. *Nature* **368**, 823–828.

Chamberlin, N. L., Traub, R. D. & Dingledine, R. (1990). Role of EPSPs in initiation of spontaneous synchronized burst firing in rat hippocampal neurons bathed in high potassium. *Journal of Neurophysiology* **64**, 1000–1008.

Flores-Hernández, J., Galarraga, E., Pineda, J. C. & Bargas, J. (1994). Patterns of excitatory and inhibitory synaptic transmission in the rat neostriatum as revealed by 4-AP. *Journal of Neurophysiology* **72**, 2246–2256.

Gulyás, A. I., Miles, R., Hájos, N. & Freund, T. F. (1993*a*). Precision and variability in postsynaptic target selection of inhibitory cells in the hippocampal CA3 region. *European Journal of Neuroscience* **5**, 1729–1751.

Gulyás, A. I., Miles, R., Sik, A., Tóth, K., Tamamaki, N. & Freund, T. F. (1993*b*). Hippocampal pyramidal cells excite inhibitory neurons through a single release site. *Nature* **366**, 683–687.

Gutnick, M. J. & Prince, D. A. (1972). Thalamocortical relay neurons: antidromic invasion of spikes from a cortical epileptogenic focus. *Science* **176**, 424–426.

Haas, H. L. & Jefferys, J. G. R. (1984). Low-calcium field burst discharges of CA1 pyramidal neurones in rat hippocampal slices. *Journal of Physiology* **354**, 185–201.

Ives, A. E. & Jefferys, J. G. R. (1990). Synchronization of epileptiform bursts induced by 4-aminopyridine in the in-vitro hippocampal slice preparation. *Neuroscience Letters* **112**, 239–245.

Kocsis, J. D., Ruiz, J. A. & Waxman, S. G. (1983). Maturation of mammalian myelinated fibers: changes in action-potential characteristics following 4-aminopyridine application. *Journal of Neurophysiology* **50**, 449–463.

Lee, W.-L. & Hablitz, J. J. (1990). Effect of APV and ketamine on epileptiform activity in the CA1 and CA3 regions of the hippocampus. *Epilepsy Research* **6**, 87–94.

Miles, R. (1990). Synaptic excitation of inhibitory cells by single CA3 hippocampal pyramidal cells of the guinea-pig *in vitro*. *Journal of Physiology* **428**, 61–77.

Miles, R., Tóth, K., Gulyás, A. I., Hajos, N. & Freund, T. F. (1994). Different functions for dendritic and somatic inhibitory cells of the hippocampus. *Journal of Physiology* **480.P**, 32*P*.

Miles, R. & Wong, R. K. S. (1987). Inhibitory control of local excitatory circuits in the guinea-pig hippocampus. *Journal of Physiology* **388**, 611–629.

Miles, R., Wong, R. K. S. & Traub, R. D. (1984). Synchronized afterdischarges in the hippocampus: contribution of local synaptic interactions. *Neuroscience* **12**, 1179–1189.

Otis, T. S., De Koninck, Y. & Mody, I. (1993). Characterization of synaptically elicited $GABA_B$ responses using patch-clamp recordings in rat hippocampal slices. *Journal of Physiology* **463**, 391–407.

Pearce, R. A. (1993). Physiological evidence for two distinct $GABA_A$ responses in rat hippocampus. *Neuron* **10**, 189–200.

Perreault, P. & Avoli, M. (1991). Physiology and pharmacology of epileptiform activity induced by 4-aminopyridine in rat hippocampal slices. *Journal of Neurophysiology* **65**, 771–785.

Perreault, P. & Avoli, M. (1992). 4-Aminopyridine-induced epileptiform activity and a GABA-mediated long-lasting depolarization in the rat hippocampus. *Journal of Neuroscience* **12**, 104–115.

Rutecki, P. A., Lebeda, F. J. & Johnston, D. (1987). 4-Aminopyridine produces epileptiform activity in hippocampus and enhances synaptic excitation and inhibition. *Journal of Neurophysiology* **57**, 1911–1924.

Stasheff, S. F., Anderson, W. W., Clark, S. & Wilson, W. A. (1989). NMDA antagonists differentiate epileptogenesis from seizure expression in an *in vitro* model. *Science* **245**, 648–651.

Stasheff, S. F., Hines, M. & Wilson, W. A. (1993*a*). Axon terminal hyperexcitability associated with epileptogenesis in vitro. I. Origin of ectopic spikes. *Journal of Neurophysiology* **70**, 960–975.

Stasheff, S. F., Mott, D. D. & Wilson, W. A. (1993*b*). Axon terminal hyperexcitability associated with epileptogenesis in vitro. II. Pharmacological regulation by NMDA and $GABA_A$ receptors. *Journal of Neurophysiology* **70**, 976–984.

Stasheff, S. F. & Wilson, W. A. (1990). Increased ectopic action potential generation accompanies epileptogenesis in vitro. *Neuroscience Letters* **111**, 144–150.

Storm, J. (1988). Temporal integration by a slowly inactivating $K^+$ current in hippocampal neurons. *Nature* **336**, 379–381.

Traub, R. D. & Dingledine, R. (1990). Model of synchronized epileptiform bursts induced by high potassium in CA3 region of rat hippocampal slice. Role of spontaneous EPSPs in initiation. *Journal of Neurophysiology* **64**, 1009–1018.

Traub, R. D., Jefferys, J. G. R., Miles, R., Whittington, M. A. & Tóth, K. (1994*a*). A branching dendritic model of a rodent CA3 pyramidal neurone. *Journal of Physiology* **481**, 79–95.

Traub, R. D., Jefferys, J. G. R. & Whittington, M. A. (1994*b*). Enhanced NMDA conductance can account for epileptiform activity induced by low $Mg^{2+}$ in the rat hippocampal slice. *Journal of Physiology* **478**, 379–393.

Traub, R. D. & Miles, R. (1991). *Neuronal Networks of the Hippocampus*. Cambridge University Press, New York.

Traub, R. D. & Miles, R. (1995). Pyramidal cell-to-inhibitory cell spike transduction explicable by active dendritic conductances in inhibitory cell. *Journal of Computational Neuroscience* (in the Press).

Traub, R. D., Miles, R. & Jefferys, J. G. R. (1993). Synaptic and intrinsic conductances shape picrotoxin-induced synchronized after-discharges in the guinea-pig hippocampal slice. *Journal of Physiology* **461**, 525–547.

Whittington, M. A., Traub, R. D. & Jefferys, J. G. R. (1995). Erosion of inhibition contributes to the progression of low magnesium bursts in rat hippocampal slices. *Journal of Physiology* **486**, 723–734.

**Acknowledgements**

This work was supported by IBM and The Wellcome Trust. J.G.R.J. is a Wellcome Trust Senior Lecturer. We wish to acknowledge critical help with using the SP1 computer from R. Walkup and J. Jann, and helpful discussions with W. A. Wilson, R. K. S. Wong, R. Miles, H. Michelson and B. Strowbridge. Drs Michelson, Wong and Strowbridge first drew our attention to the fact that 4-AP-induced after-discharges were not dependent on NMDA receptors.

*Received 19 December 1994; accepted 25 May 1995.*